Imaging Covalent Bonding between Two NO Molecules on Cu(110)

A. Shiotari, Y. Kitaguchi, and H. Okuyama*

Department of Chemistry, Graduate School of Science, Kyoto University, Kyoto 606-8502, Japan

S. Hatta and T. Aruga

Department of Chemistry, Graduate School of Science, Kyoto University, Kyoto 606-8502, Japan
JST CREST, Saitama 332-0012, Japan
(Received 23 January 2011; published 14 April 2011)

Using a scanning tunneling microscope, we found metastable upright NO on Cu(110) with the $2\pi^*$ molecular resonance at the Fermi level. Upon heating above 40 K, it converts to a bent structure with the loss of molecular resonance. By manipulating the distance between two upright NO, we controlled the overlap between $2\pi^*$ orbitals and observed its splitting below and above the Fermi level, thus visualizing the covalent interaction between them.

PACS numbers: 68.37.Ef

The interaction between adsorbed molecules plays an important role in many surface phenomena such as diffusion and catalysis. The direct interaction via the overlap of the molecular orbital is of particular interest with relevance to the associative combination and reaction between adsorbates. Nitric oxide (NO) has an unpaired electron in its $2\pi^*$ orbital, and this could give rise to a covalent interaction between two NO molecules on the surface to form a dimer as in a gas phase [1] and in a matrix [2]. Upon adsorption on metal surfaces, however, the $2\pi^*$ orbital of NO is usually hybridized with surface electronic states [3–5] so that the unpaired electron is delocalized in the metal, resulting in the loss of the paramagnetism [6]. On the other hand, the $2\pi^*$ orbital was suggested to be mostly retained on Cu and Ag surfaces [7,8], where the surface d bands are located far below the Fermi level and thus the interaction is weak enough for NO to retain its molecular character. On these surfaces, covalent interaction could contribute between NO molecules via the overlap of the "active" $2\pi^*$ molecular orbitals. Actually, dimerization of NO has been observed in the submonolayer regime on Cu [9,10] and Ag [11,12]. Nevertheless, it remains yet to be clarified if the $2\pi^*$ molecular state is indeed present for an isolated NO monomer and then how it evolves as NO forms a dimer.

The scanning tunneling microscope (STM) can probe the electronic states of individual atoms and molecules on metal surfaces. Combined with manipulation techniques, it has been used to investigate the effect of adatom-adatom interaction on the electronic states of assembled dimer and extended chains [13–15]. Here, we characterized the valence states of individual NO molecules on Cu(110) by using an STM and found that $2\pi^*$ molecular resonance exists at the Fermi level when it is weakly bound on the surface. By decreasing the distance between two NO molecules with the STM, we observed overlap between $2\pi^*$ orbitals and the appearance of new states below and above the Fermi level, that correspond to bonding and antibonding orbital formation, respectively.

The experiments were carried out in an ultrahigh-vacuum chamber equipped with an STM operating at 6 K. An electrochemically etched tungsten tip was used as an STM probe. The STM images were acquired in the constant current mode at the sample bias $V = 30$ mV and tunneling current $I = 0.5$ nA. A single crystalline Cu(110) was cleaned by repeated cycles of argon ion sputtering and annealing. The clean Cu(110) surface was exposed to NO gas at 12 K. Scanning tunneling spectroscopy (STS, dI/dV) was conducted by using a lock-in amplifier with a modulation of 4 mV$_{rms}$ at 590 Hz. The tip height was fixed over the molecule at $I = 0.5$ nA and $V = 30$ mV. The spectrum recorded over the clean surface at the same tip-surface distance was subtracted from each of the STS data.

Figure 1(a) shows typical STM images of individual NO molecules on Cu(110). Each molecule appears as two protrusions aligned along the Cu row ([1$\bar{1}$0] direction). The grid lines represent the lattice of Cu atoms on the surface, suggesting that a NO molecule is bonded to the short-bridge site on the Cu row with an upright configuration. The adsorption site was determined from the relative position of NO molecules to OH groups which are known to be adsorbed on the short-bridge site [16,17]. The dumbbell-shaped image reflects the shape of the $2\pi^*$ orbital of upright NO [Fig. 1(b)], implying that it mainly contributes to the tunneling and thus dominates the density of states at the Fermi level.

STS was conducted with the tip fixed over one of the protrusions [solid curve in Fig. 1(c)]. The STS shows a peak centered at the Fermi level with the width of ~ 200 mV. The spatial maps of the STS intensities were recorded at -200 [Fig. 1(d)], -80 [Fig. 1(e)], and 200 mV [Fig. 1(f)]. During the mappings, the tip height was fixed so that the current was $I = 0.5$ nA at $V = 30$ mV over the protrusion. The spatial distributions at these voltages all
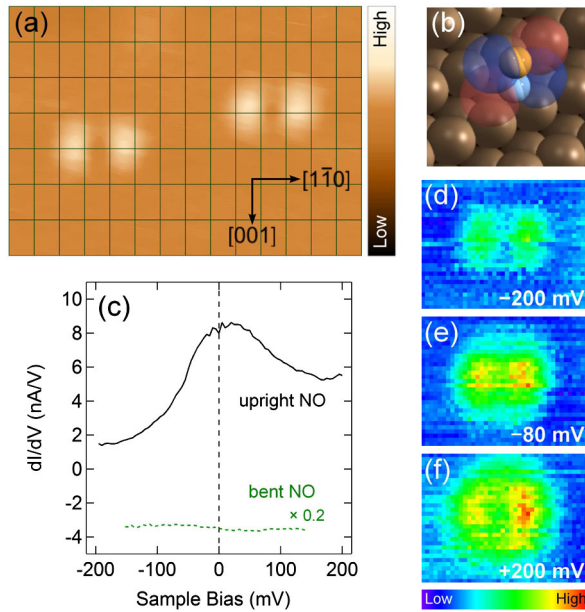
FIG. 1 (color online). (a) Typical STM images of NO on Cu(110) (36×25 Å^2, $V = 30$ mV, and $I = 0.5$ nA). The lines represent the lattice of surface Cu atoms. (b) Schematic illustrations of the bonding structure and $2\pi^*$ orbital of NO. It adsorbs upright on a short-bridge site via the N atom. The dumbbell-shaped image implies that the $2\pi^*$ state mainly contributes to the tunneling. (c) The STS recorded over the protrusion of the dumbbell-shaped image (solid curve). A broad peak was observed at the Fermi level. The dashed curve shows the STS recorded over dark NO [Fig. 2(a)], showing no feature around the Fermi level. (d) dI/dV spatial map at $V = -200$ mV for the dumbbell-shaped image. The tip height was fixed during the data acquisition so that $I = 0.5$ nA and $V = 30$ mV over the protrusions. (e) dI/dV spatial maps at $V = -80$ mV and (f) at $V = 200$ mV taken in a similar way as (d). The spatial distributions show the shape of $2\pi^*$ molecular orbital, indicating that the broad STS peak in (c) is assigned to the $2\pi^*$ resonance. The image size in (d)–(f) is 13×10 Å^2.

show the shape of the $2\pi^*$ orbital of upright NO, indicating that the broad STS peak at the Fermi level is assigned to $2\pi^*$ molecular resonance. The peak is broadened due to the hybridization with the substrate. The hybridization is also manifest in the large distance between the protrusions (2–6 Å depending on the tunnel condition), compared to that of the intact $2p$ orbital.

Upon heating to 40 K, the dumbbell-shaped protrusion converts to a round depression [Fig. 2(a)]. The depression is displaced from the exact short-bridge site in the [001] or [00$\bar{1}$] direction and thus is assigned to bent NO with the axis tilted along [001], that was previously observed by vibrational spectroscopies [10,18]. The dark image reflects that the $2\pi^*$ molecular resonance is no longer retained for the bent species, as confirmed by its disappearance in the STS recorded over the depression [dashed curve in Fig. 1(c)]. The $2\pi^*$ orbital is strongly hybridized with the surface, giving rise to the shift far away from the Fermi level. It was observed to split at ~2 eV below and above the Fermi level on Ni and Pd surfaces by (inverse)
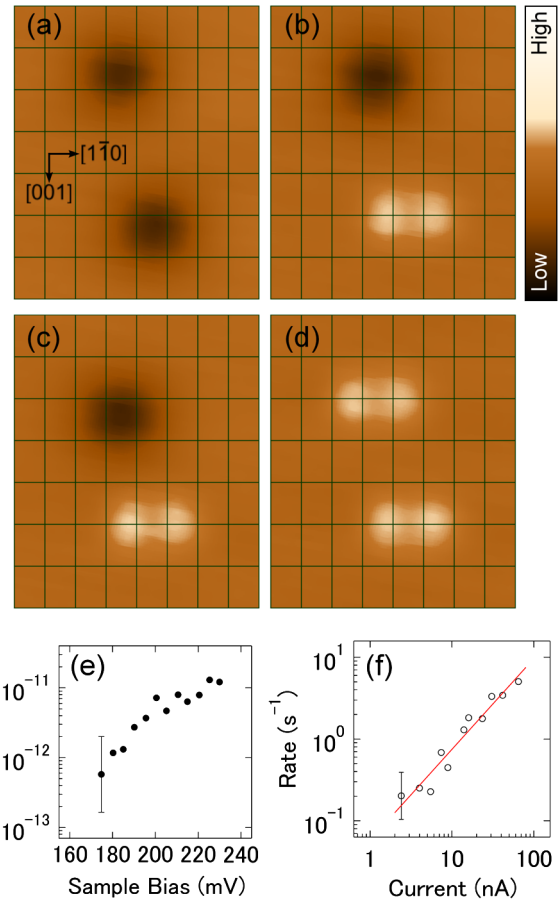
FIG. 2 (color online). (a) Typical STM images of NO molecules adsorbed at 40 K. They are imaged as a round depression displaced from the short-bridge site in the [001] or [00$\bar{1}$] direction. The displacement is ascribed to the tilt of the molecular axis (bent NO). (b) By applying a voltage pulse of 0.2 V to bottom bent NO in (a), it converted to an upright species imaged as a dumbbell-shaped protrusion. (c) A voltage pulse of 0.2 V to top bent NO in (b) induced the flip of the axis. (d) Another pulse to top bent NO in (c) induced the conversion into the upright configuration. The image size in (a)–(d) is 20×25 Å^2, and they were obtained at $V = 30$ mV and $I = 1$ nA. (e) The reaction yield determined from averaging the conversion time as a function of voltage. 15 bent NO molecules were used to determine the yield for each voltage. The tip was fixed over the depression with the height adjusted so that the current during the pulse (before the reaction) was 40 nA. (f) The current dependence of the conversion rate at $V = 230$ mV in a logarithmic scale. The slope is 1.1 ± 0.3, suggesting that the conversion proceeds via a one-electron process. The vertical bars in (e) and (f) show the variation with the tip apex.

photoemission spectroscopies [3–5]. Thus, we found that there exist two adsorbed states of NO on Cu(110): One is a weakly bound upright species with the $2\pi^*$ molecular resonance located at the Fermi level, and the other is a more stable bent species which no longer retains the molecular character due to significant hybridization with the substrate.

The bent species could be converted to the upright one by injecting tunneling electrons with the STM. By applying a voltage pulse of 0.2 V over bent NO

[bottom in Fig. 2(a)], it turned into an upright configuration [Fig. 2(b)] that showed the same $2\pi^*$ molecular resonance as Fig. 1(c). Alternatively, the bent axis flipped to the other direction by a similar voltage pulse. A voltage pulse of 0.2 V to another bent NO [top in Fig. 2(b)] induced flip of the axis [Fig. 2(c)]. It was subsequently converted to the upright configuration by a second pulse [Fig. 2(d)]. The conversion was more frequent than the flip by a factor of ~ 10. We confirmed that the manipulated upright species turned back into the bent structure upon annealing to 40 K. The upright turning was investigated as a function of the pulse voltage [Fig. 2(e)] and tunneling current [Fig. 2(f)]. The conversion starts to be observed around $V = 180$ mV, and the yield gradually increases with the voltage. With negative sample bias, a similar increase of the yield was observed. The current dependence suggests a one-electron process. By infrared absorption spectroscopy for NO/Cu(110) at 40 K, the N-O stretch mode for isolated bent species was observed at ~ 200 meV [10]. Therefore we suggest that excitation of the internal mode by tunneling electrons is responsible for the conversion from the "stable" bent to "metastable" upright configurations. The internal mode decays via anharmonic coupling to external modes leading to the motion or transformation of the molecule [19,20]. On the other hand, the reverse reaction from the upright to bent configuration was not feasible by tunneling electrons. The upright species instead migrated along the Cu row under a voltage of ~ 0.2 V. This one-way conversion to a less stable upright structure is associated with nonthermal activation by tunneling electrons.

The existence of the molecular resonance at the Fermi level suggests that covalent interaction may exist between two upright NO molecules via the overlap of the $2\pi^*$ orbitals modified by the substrate. Two NO molecules were located along the same Cu row [Fig. 3(a)] with the intermolecular distance of $4a_0$ ($a_0 = 2.56$ Å is the Cu atomic distance along the row). The lateral manipulation of a NO molecule was conducted by positioning the tip over a molecule at reduced tip-surface distance (~ 0.1 MΩ gap resistance) and then moving it at 1 Å/s along the Cu row with the feedback maintained [16,21]. An upright NO molecule [left in Fig. 3(a)] was brought toward another (right) so that the intermolecular distance is $3a_0$ [Fig. 3(b)], $2a_0$ [Fig. 3(c)], and a_0 [Fig. 3(d)]. We note that upright NO does not convert to bent NO under any bias or current, ensuring that the latter is not involved in this experiment. The corresponding profiles of topographic height along the two NO molecules are shown in Fig. 3(e). At the distances of $4a_0$ and $3a_0$, two NO molecules appear as they are almost independent of each other, and the apparent height is similar to that of an isolated NO molecule (0.18 Å). On the other hand, when the distance is reduced to $2a_0$, one-side protrusion is overlapped between two NO molecules and they appear as three protrusions [Fig. 3(c)]. Among them, the outer ones appear more protruded (0.21 Å), suggesting that the electronic
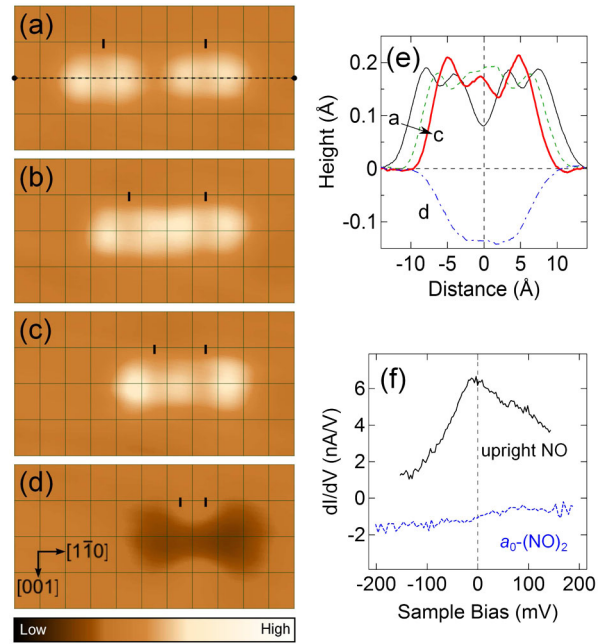
FIG. 3 (color online). (a) STM images of two upright NO molecules located along the same Cu row. By laterally manipulating the left molecule in (a), we varied the intermolecular distance and induced the overlap between the $2\pi^*$ molecular orbitals. The distance is (a) $4a_0$, (b) $3a_0$, (c) $2a_0$, and (d) a_0, where $a_0 = 2.56$ Å is the Cu atomic distance along the row. The solid lines show the lattice of surface Cu atoms, and the tick marks indicate the lateral positions of the molecules. The image size is 28×14 Å^2. (e) The profiles of the topographic height across the two molecules in (a)–(d), as shown by the dashed line in (a). They are shown from -15 to 15 Å with respect to the center between the two molecules. (f) The STS recorded over the protrusion of an isolated NO (solid curve) and that recorded over the depression of $a_0 - (NO)_2$ in (d) (dashed curve). At the distance of a_0, the $2\pi^*$ resonance is quenched due to the strong overlap.

structure near the Fermi level is changed due to NO-NO interaction. Further reduction of the distance to a_0 resulted in complete quenching of the protrusions and the appearance of a characteristic depression [Fig. 3(d)]. The corresponding STS showed no density of states near the Fermi level [dashed curve in Fig. 3(f)], in contrast to the peak for isolated monomers [solid curve in Fig. 3(f)]. This is attributed to the strong overlap between two $2\pi^*$ orbitals, resulting in the formation of bonding and antibonding states far from the Fermi level. It appears as a characteristic depression of C_{2v} symmetry and probably consists of two NO molecules bonded to the neighboring short-bridge sites. It could be reversely dissociated into two upright monomers along the row by applying an ~ 0.7 V pulse.

Two NO molecules are interacted even at the distance of $2a_0$ [Fig. 3(c), $2a_0$-$(NO)_2$]. The corresponding STS showed broad peaks at ~ -30 and ~ 20 mV [Fig. 4(a)] when the tip was fixed over the center and outer protrusions, respectively, while it is centered at the Fermi level for an isolated monomer (dashed curve). We recorded these spectra with the same tip apex to confirm the peak shifts between them.
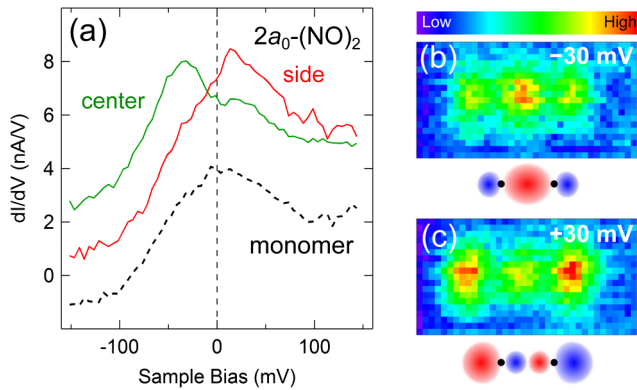
FIG. 4 (color online). (a) The STS recorded over the center and side protrusions of $2a_0 - (NO)_2$ in Fig. 3(c). For comparison, the STS recorded over an isolated species is also shown (dashed curve, vertically offset for clarity). These spectra were obtained with the same tip apex. The $2\pi^*$ resonances of $2a_0 - (NO)_2$ appear below and above the Fermi level, indicating the energy splitting by covalent interaction between two NO molecules. The STS spatial maps recorded at (b) -30 and (c) 30 mV demonstrate the shape of bonding and antibonding orbitals, respectively. The inset shows schematically the bonding and antibonding orbitals formed by σ bonding between two $2p$ orbitals. The STS data and the spatial maps were obtained at the same height corresponding to $I = 0.5$ nA and $V = 30$ mV over the outer protrusion. The image size is 20×10 Å^2.

The STS spatial distributions for $2a_0$-$(NO)_2$ were recorded at -30 [Fig. 4(b)] and 30 mV [Fig. 4(c)] at a constant height. The intensities are largest over the center and outer protrusions at $V = -30$ and 30 mV, respectively. The former and the latter show the shape of the bonding and antibonding orbitals (depicted in the inset), respectively, which arise from the overlap of the $2\pi^*$ molecular resonance originally centered at the Fermi level. Note that the node at the molecular center for the antibonding orbital was not observed due to the partial contribution from the bonding orbital (The STS mapping recorded at the ~ 20 mV peak was also contributed from the ~ -30 mV peak and vice versa due to the large peak widths). The antibonding orbital is also seen in the topographic image recorded at $V = 30$ mV [Fig. 3(c)] that shows three protrusions with the outer ones more protruded. Since the bonding and antibonding states are located near the Fermi level, their spatial features are reflected in the topographic images as well as in the dI/dV mappings [16].

The stabilization energy due to the covalent interaction can be estimated from the split energy between the bonding and antibonding states. For $2a_0$-$(NO)_2$, it is ~ 50 mV, while that of a_0-$(NO)_2$ is larger than 400 mV. The splitting for larger distances was too small to be detectable. These results indicate that the interaction decays abruptly as the distance increases, which is characteristic of a covalent interaction. The effect of interatomic coupling on the electronic states of assembled systems has been studied with STM [13–15]. Nilius et al. built Au dimers on NiAl (110) that showed the doublet states of symmetric and antisymmetric character, which is similar to our result [13]. In these previous works, however, the electronic states of interest were located far away from the Fermi level, and thus the overlap between them did not contribute to the stabilization of the system or covalent bonding.

In summary, we found metastable upright NO on Cu(110) which is only accessible at a temperature below 40 K. The weak interaction allows the molecular character to be almost retained, resulting in the survival of the open-shell $2\pi^*$ state. By manipulating the distance between two upright NO, we induced the overlap between the $2\pi^*$ orbitals and observed the formation of bonding and antibonding states below and above the Fermi level, respectively, thus controlling and visualizing a covalent interaction between two adsorbed NO molecules.

*hokuyama@kuchem.kyoto-u.ac.jp
[1] C. E. Dinerman and G. E. Ewing, J. Chem. Phys. **53**, 626 (1970).
[2] W. A. Guillory and C. E. Hunter, J. Chem. Phys. **50**, 3516 (1969).
[3] H. Conrad et al., Surf. Sci. **65**, 235 (1977).
[4] J. Rogozik, J. Küppers, and V. Dose, Surf. Sci. **148**, L653 (1984).
[5] D. E. Peebles, E Hardegree, and J. M. White, Surf. Sci. **148**, 635 (1984).
[6] W. A. Brown and D. A. King, J. Phys. Chem. B **104**, 2578 (2000).
[7] A. Yoshimori, Surf. Sci. **342**, L1101 (1995).
[8] M. P. Jigato, D. A. King, and A. Yoshimori, Chem. Phys. Lett. **300**, 639 (1999).
[9] P. Dumas et al., Surf. Sci. **371**, 200 (1997).
[10] W. A. Brown et al., J. Phys. Chem. **100**, 12 559 (1996).
[11] W. A. Brown, P. Gardmer, and D. A. King, J. Phys. Chem. **99**, 7065 (1995).
[12] C. I. Carlisle and D. A. King, J. Phys. Chem. B **105**, 3886 (2001).
[13] N. Nilius et al., Phys. Rev. Lett. **90**, 196103 (2003).
[14] S. Fölsch et al., Phys. Rev. Lett. **92**, 056803 (2004).
[15] A. Sperl et al., New J. Phys. **11**, 063020 (2009).
[16] See supplemental material at http://link.aps.org/supplemental/10.1103/PhysRevLett.106.156104 for details of the site determination of upright NO, the means of NO manipulation, and bias-dependent topographic images of $2a_0$-$(NO)_2$.
[17] T. Kumagai et al., Phys. Rev. B **79**, 035423 (2009).
[18] J. F. Wendelken, Appl. Surf. Sci. **11/12**, 172 (1982).
[19] B. C. Stipe, M. A. Rezaei, and W. Ho, Phys. Rev. Lett. **81**, 1263 (1998).
[20] T. Komeda et al., Science **295**, 2055 (2002).
[21] L. Bartels, G. Meyer, and K.-H. Rieder, Phys. Rev. Lett. **79**, 697 (1997).